ELSEVIER

Chemical Physics 189 (1994) 261–272

Chemical Physics

Adiabatic approximation and non-adiabatic effects for open-shell atoms in an inert solvent: F atoms in solid Kr

A.I. Krylov [a,b], R.B. Gerber [a,b], V.A. Apkarian [b]

[a] *Department of Physical Chemistry and The Fritz Haber Research Center for Molecular Dynamics, The Hebrew University, Jerusalem 91904, Israel*

[b] *Department of Chemistry, University of California, Irvine, CA 92717, USA*

Received 17 June 1994

Abstract

The dynamics of P-state F atoms in solid Kr is studied by molecular dynamics simulations in two frameworks: (i) The adiabatic approximation, in which nuclear motion is confined to the lowest adiabatic potential surface of the system; (ii) A method that treats semiclassically non-adiabatic transitions between electronic states in the course of the dynamics. The simulations deal with the spectroscopy of the F atom at different lattice sites, and with orbital reorientation dynamics due to the coupling with lattice vibrations. Also explored is migration of the F atom, following the preparation of an exciplex $Kr_2^+ F^-$ which dissociates radiatively in the lattice. Some of the main findings are: (1) p-orbital reorientation dynamics on very short timescales ($t \lesssim 20$ fs) is dominated by non-adiabatic mechanisms. Adiabatically, reorientation effects have timescales of the order of 0.25 ps or longer. (2) Lattice vibrations of particular symmetry types are particularly efficient in inducing p-orbital reorientation. (3) Dissociation of a $Kr_2^+ F^-$ exciplex can result in migration of the F atom into several lattice sites. The F atom spectroscopy for the different sites is different, and can be experimentally distinguished. (4) The migration probabilities of the F atom calculated adiabatically are much greater than the non-adiabatic ones. The results shed light on the coupling between electron orbital and nuclear dynamics for P-state atoms in solids.

1. Introduction

The study of open-shell atoms in rare-gas solids is a convenient framework for exploring a very basic question, namely what is the effect of the solvent on the dynamics of an electron orbital immersed in it. The issue is particularly interesting in cases where a P or D state atom is involved, since then electronic degeneracy or near-degeneracy arises, and the possible breakdown of the Born–Oppenheimer approximation must be addressed. The present article explores the dynamics of a p-type orbital and its coupling to the motions of the nuclei for a guest F atom in a host rare-gas solid.

Experimentally, open-shell atoms in solid matrices are a widely studied field. Examples of spectroscopic studies of impurity atoms in rare-gas solids, related to the topics of the present article, are found in Refs. [1–8]. The focus in theoretical work in this area so far has been mostly on the interpretation of the electronic spectroscopy. In particular, Balling and Wright developed a treatment for the interpretation of the structure seen in the electronic spectra of alkali atoms isolated in rare gas solids [9]. Their approach was based on the role of electrostatic interactions with lattice atoms in split-

SSDI 0301-0104(94)00322-X

ting the degenerate P-state excited levels of the alkali atom. Monte Carlo calculations by Fajardo and coworkers [10,11] on alkali atom spectra in matrices demonstrated the influence of different guest atom sites in the spectroscopy. Fajardo et al. [11] showed that absorption spectra following deposition of very energetic alkali atoms can differ considerably, due to the sites occupied in this case, from the corresponding behavior in thermal deposition. Danylichev and Apkarian presented the adiabatic potential energy surfaces for $O(^1S)$, $O(^1D)$ and $O(^3P)$ in Kr and Xe crystals, and reproduced by Monte Carlo simulations the site specific spectra of $O(^1S) \rightarrow O(^1D)$ transition [8b]. Lawrence and Apkarian treated the $I^* \rightarrow I$ spin–orbit transitions in Kr and Xe, and showed that with minor corrections to pair parameters ($\sim 3\%$) these Jahn–Teller split spectra could be reproduced in the limit of adiabatic following Ref. [8c]. Likewise, theoretical simulations of electronic absorption spectra of large Ba–$(Ar)_n$ clusters by Visticot et al. [12] proved very successful in accounting for the experimental findings in these systems. However, these theoretical studies and simulations have not attempted to deal with the role and dynamics of *non-adiabatic* effects in such systems. Indeed, only very few theoretical studies touch on this issue, and very little is known on the mechanisms and timescales involved. Benjamin and Wilson carried out molecular dynamics (MD) simulations that include the role of *intramolecular* non-adiabatic transitions in the photolysis of ICN in Ar [13]. Non-adiabatic transitions due to the interactions of the photoproducts with the solvent were, however, not treated. Nearest to our perspective here is the paper by Gersonde and Gabriel [14] who carried out MD simulations, including a treatment of non-adiabatic transitions, for photodissociation and recombination of molecules such as HCl and Cl_2 in rare-gas solids.

The basic aim of the present article is to explore the dynamics of a P-state guest atom in a host lattice, including the role of the coupling between electronic and nuclear motions. An $F(^2P)$ atom in solid Kr will be used as a realistic model system. A major objective in this framework is to explore the dynamics in the limit of the Adiabatic Approximation, and to determine its shortcomings and the scope of its applicability. The adiabatic (or Born–Oppenheimer) approach will be carried out by an algorithm that treats the determination of the electronic potential surfaces "on the fly", as the dynamics of the atomic motion evolves. The Adiabatic MD simulation will be compared with MD simulations that include non-adiabatic transitions, treated by a semiclassical surface hopping method. In this way we aim to compare, for instance, the mechanisms and rates of p-orbital reorientation in the solid, in the adiabatic and non-adiabatic frameworks, respectively. We propose to explore the combined electronic-orbital/nuclear dynamics for a substitutional $F(^2P)$ atom in Kr, in thermal conditions, and also for a process in which an exciplex $Kr_2^+ F^-$ dissociates radiatively in the solid. The latter will lead us to photoinduced migration events for the F atom into different sites, and to comparison of the adiabatic and non-adiabatic dynamics for the migration process.

The structure of this article is as follows: In Section 2 we discuss the modelling of the system, and in particular the interaction potentials used. Section 3 presents the methods employed here for the dynamics, both the "on the fly" adiabatic MD algorithm, and the non-adiabatic simulation method. Section 4 presents results on the dynamics and spectroscopy of an F atom in a substantial site of a Kr lattice. Section 5 gives the results for dissociation of a $Kr_2^+ F^-$ exciplex in solid Kr. Concluding remarks are brought in Section 6.

2. System and interaction potentials

The model system studied in this paper is an $F(^2P)$ atom embedded in a very large cluster of Kr atoms. The number of rare-gas atoms used in the calculations [25] was large enough for the results not to be significantly affected by the finite size of the model system. Periodic boundary conditions were imposed at the edges of the cluster, to correspond to the realistic case of an isolated F atom guest in a Kr lattice.

The total potential function of the system was taken to be of the form

$$V = \sum_i U_i + \sum_{i>j} u(r_{ij}) \,, \tag{1}$$

$u(r_{ij})$ in the second term of Eq. (1) is the pair potential between the i and j Kr atoms. For the $u(r)$ pair potential between Kr atoms, we employed the potential of Aziz and Slaman [15], which was fitted accurately to spectroscopy, scattering and dilute gas data. Our treatment ignores three-body forces among the rare-gas atoms, as

we estimate that the latter are unlikely to be important enough to affect the properties of interest here. We assume also pairwise atom–atom interactions between the fluorine and each of the krypton atoms. For the F/Kr interaction we used the potential determined by Becker, Casavecchia and Lee [16] from their molecular beam scattering data. The interaction U_i between the F and the ith Kr atom can be written

$$U_i = V_0(r_i) + V_2(r_i)P_2(\cos\gamma_i)\ , \qquad (2)$$

where the functions $V_0(r)$, $V_2(r)$ are given in Ref. [16]. r_i denotes the distance between F and the ith Kr atom. The angle γ_i is interpreted as a coordinate associated with the open-shell electrons. Using a single effective electron model for the open-shell of $F(^2P)$, and in a semiclassical framework, γ_i can be considered as the angle between this electron and the F–Kr axis. Since U_i contains an electronic degree of freedom, it does not correspond to a potential function in the Born–Oppenheimer sense. Interactions of the form of Eq. (2) between ^2P and S-state atoms have been accurately determined from molecular beam experiments for a number of systems in recent years [16,17]. The theoretical background for using these potentials is discussed in Refs. [18,19,9]. It should be noted that in using the interaction of Eqs. (1), (2) for a polyatomic system, as in the present case, one ignores three- and higher-order many body interactions between the open shell atom and the solvent atoms. The interactions of the F atom with the rare gas atoms so constructed are at the pairwise level only. The accuracy of such potentials, and in particular the pairwise additive assumption implied by Eq. (1) were demonstrated in Refs. [8b] and [8c] to be quite satisfactory at least in stable trapping sites and at thermal energies. Their validity in describing the entire surface and in particular saddle points deserves careful future attention, but represents the best available model at present.

In calculations of the dynamics, the interaction V is represented in a basis of orbitals, which represent the single effective open-shell electron. Introducing an external coordinate system for the solid with the atom in it, the basis set we use to represent the electron is p_x, p_y, p_z. Using the functional forms of these orbitals (only the angular dependence is required in our model), and Eq. (2), one can readily obtain both the diagonal and the non-diagonal elements V_{ij} of V in Eq. (1), where i, $j = \{p_x, p_y, p_z\}$. The V_{ij} are functions only of the nuclear

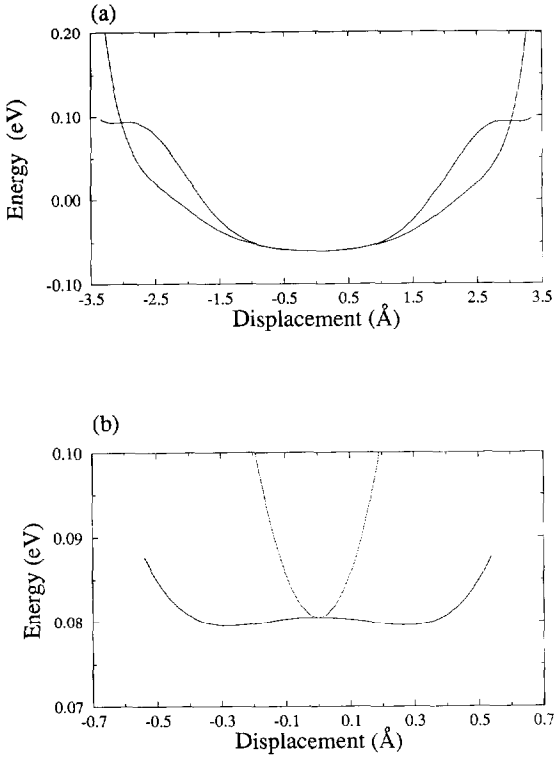

Fig. 1. (a) Adiabatic potential functions for the displacement of F along the x-axis in a substitutional site in a Kr lattice. (b) Adiabatic potential functions for the displacement of F along the x-axis in an O_h interstitial site in Kr.

positions of the F and of the Kr atoms, $\boldsymbol{r}_1, \ldots, \boldsymbol{r}_N$, where N is the number of atoms in the system. In the *adiabatic* approximation, the potential matrix $V_{ij}(\boldsymbol{r}_1, \ldots, \boldsymbol{r}_N)$ is diagonalized, and nuclear motions are confined to a single adiabatic potential surface. (We shall describe later an algorithm for determining the adiabatic potential surfaces and the corresponding electronic states "on the fly", as the trajectories of the system are propagated). The adiabatic potential surfaces will be denoted by V_1^a, V_2^a, V_3^a. It will be useful for the purpose of gaining insight into the dynamics later, to note some of the properties of these potential surfaces for our system.

Consider first the case where the F atom occupies a substitutional site in the Kr solid. Fig. 1a shows the adiabatic potentials for the system when all the Kr atoms occupy perfect fcc lattice positions, and the F atom is displaced from its equilibrium position along (001) direction of the system to which we refer below

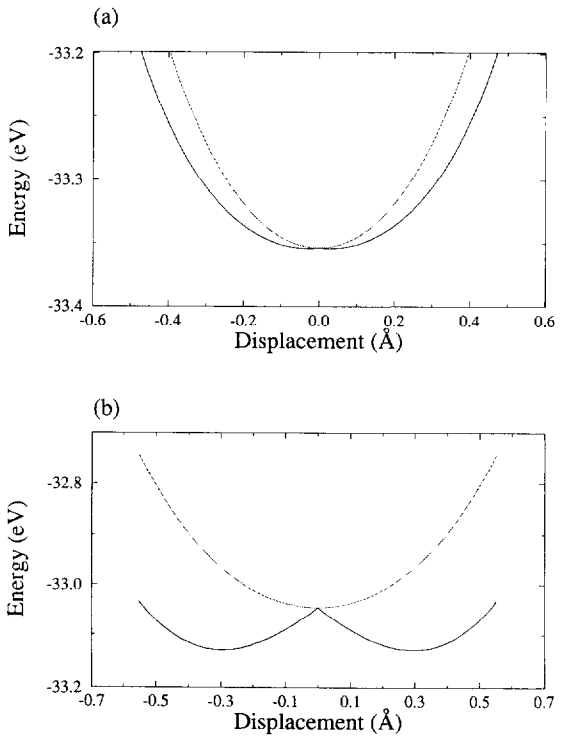

Fig. 2. (a) Adiabatic potentials vs. an asymmetric distortion of the cage for F in an O_h interstitial site in Kr. (b) Adiabatic potentials versus an asymmetric distortion of the cage for F in a T_d interstitial site in Kr.

as the x-axis. For such displacements, there is a two-fold degeneracy $V_2^a(\boldsymbol{r}) = V_3^a(\boldsymbol{r})$. The curves do not exhibit a conical intersection structure, since the shifting of the F atom along the x-axis is not a Jahn–Teller degeneracy removing mode. The adiabatic potentials for this displacement when the F atom is at a substitutional site are harmonic and shallow near the origin. Fig. 1b shows the corresponding behavior of the potentials in the case where the F atom is at an interstitial O_h site. The Kr atoms are again placed at perfect lattice positions, and the F is displaced in the x direction (001). Also in this case $V_2^a = V_3^a$ by symmetry. Note that for this site, V_1^a has a very shallow double well structure along the displacement, while V_2^a is steep and harmonic. Although the potential energy curves look like JT splitting, in reality a quadratic effect is presented. Fig. 2a is again for an F atom at an O_h interstitial site in the Kr lattice, but in this case the displacement considered is a Jahn–Teller degeneracy lifting vibration, corresponding to an asymmetric vibration of the cage (E_{2g} modes). There is a barely noticeable Jahn–Teller behavior for V_1^a and V_2^a in this case. However, the effect is very weak. Fig. 2b shows V_1^a, V_2^a as a function of an asymmetric cage vibration when the F atom is at an interstitial T_d site. In this case the JT active mode corresponds to and E-type vibration of the tetrahedron. In this case, a pronounced Jahn–Teller splitting structure is seen. This is obviously a consequence of the fact that the T_d site is more compressed, and the interactions of the F atom with the crystal are much stronger. Figs. 1 and 2 point to two important features of the system studied: The behavior for different sites should be very different, and electronic degeneracy and Jahn–Teller effects are expected to play a very major role.

In considering the state and interactions for this system, we ignored spin–orbit coupling effects. This is justified for an F atom in rare-gas media, although the situation for the heavier halogens is quite different. The spin–orbit split states of iodine were discussed in depth in Ref. [8c]. Spin–orbit coupling was found to play a major role for the dynamics of $Cl(^2P)$ in solid Ar [20].

3. Methods for simulating the dynamics

3.1. Molecular dynamics in the adiabatic approximation by an "on the fly" algorithm

In this approach, nuclear motions are assumed to be confined to a single adiabatic potential energy surface, e.g. the lowest adiabatic surface. The implementation of the method is straightforward. Suppose that at time t we have the state of the system: the configuration $\boldsymbol{r}(t) = \boldsymbol{r}_1(t), \ldots, \boldsymbol{r}_N(t)$ of the atoms and their velocities; the adiabatic potential $V_1^a(\boldsymbol{r}(t))$ on which the atoms move; and the electronic wavefunction which describes the single effective electron assumed to model the open-shell of the F. The electronic wavefunction can be written

$$\psi(\theta, \phi, t) = C_1^1(t)\mathrm{p}_x + C_2^1(t)\mathrm{p}_y + C_3^1(t)\mathrm{p}_z\,, \qquad (3)$$

where θ, ϕ are orientation angles in the external coordinate system of an axis from the F nucleus to the instantaneous position of the effective electron. To propagate the system to time $t' = t + \Delta t$, we solve Newton's equations for the $\boldsymbol{r}_i$ on the adiabatic potential surface:

$$m_i \frac{d^2 \boldsymbol{r}_i}{dt^2} = -\nabla_{\boldsymbol{r}_i} V_1^a(\boldsymbol{r}_1, \ldots, \boldsymbol{r}_N), \quad i = 1, \ldots, N. \qquad (4)$$

Approximating the forces on the right hand side of Eq. (4), by the value of the forces at time t, we can integrate the equations for a small time-step and obtain $\boldsymbol{r}_1(t+\Delta t), \cdots, \boldsymbol{r}_N(t+\Delta t)$. The representation of the interaction $V(\boldsymbol{r}(t+\Delta t), \theta, \phi)$ of Eqs. (1) and (2) in the basis of the p-orbitals can then be computed. The 3×3 matrix obtained will be denoted $V_{ij}(\boldsymbol{r}(t+\Delta t))$, with $i,j = \{p_x, p_y, p_z\}$. Diagonalization of the latter gives $V_1^a(\boldsymbol{r}(t+\Delta t))$ (as well as the other adiabatic surfaces at $t+\Delta t$). The components of the corresponding eigenvector $(C_1^1(t+\Delta t), C_2^1(t+\Delta t), C_3^1(t+\Delta t))$ are the coefficients of the electronic wavefunction at $t' = t+\Delta t$. Using the adiabatic potential at $\boldsymbol{r}(t+\Delta t)$, one can obtain the configuration for the next time-step from Eq. (4), and so on. Thus, the electronic wavefunction and the adiabatic potential surface are calculated along and with the trajectory. The method is strictly within the Born–Oppenheimer framework. The properties of the system as described by the method can, however, differ very significantly from these systems of closed-shell, spherical atoms. The present description includes, for instance, reorientation effects of the electron orbital, although the latter occurs here strictly due to adiabatic following by the orbital of the neighboring atoms. Although the interaction potential V in Eq. (1) was constructed from pairwise atom–atom terms, the adiabatic potential surfaces $V_j^a(\boldsymbol{r}_1, \ldots, \boldsymbol{r}_N)$ are not in general pairwise functions. Indeed, effects implied by the electron orbital following dynamics can be inconsistent with a potential surface that is a sum of pairwise atom–atom potential functions [8c].

3.2. Non-adiabatic dynamics with surface hopping

There is a considerable arsenal of theoretical methods for treating non-adiabatic processes in condensed phases [21–26]. The usefulness of these methods in selected applications has been demonstrated, but there is a lack of knowledge as to the scope of validity and accuracy of each of the methods in more general applications. The approach taken here is very similar in principle, although different in some technical aspects, to Tully's method [23]. In this approach, the system can "hop" from one potential surface to another, according to a probability function for such non-adiabatic transitions that is evaluated along the dynamical evolution. Between hopping events, the atomic nuclei propagate on a given potential surface according to classical dynamics. Tully's method can be introduced for adiabatic or for diabatic states, depending on the physical advantages for a given system [23]. We introduce here the method for the crude basis of p-orbitals, p_x, p_y, p_z. When the electronic state is described by one of these orbitals, p_k, the potential surface that governs nuclear motions is, using Eq. (1):

$$V_{kk}(\boldsymbol{r}_1, \ldots, \boldsymbol{r}_N) = \sum_i \langle p_k | U_i | p_k \rangle + \sum_{i>j} u(r_{ij}). \qquad (5)$$

As long as a non-adiabatic transition to another surface has not occurred, nuclear dynamics is propagated according to $V_{kk}(\boldsymbol{r})$. Let $\boldsymbol{r}(t)$ denote the trajectory of the atom on this potential. Substituting the trajectory function in Eq. (2), one obtains a time-dependent interaction that acts on the electronic degrees of freedom:

$$U(t; \theta, \phi) \equiv \sum_i U_i(\boldsymbol{r}(t); \theta, \phi) . \qquad (6)$$

To obtain a criterion for the occurrence of a non-adiabatic transition, we expand the perturbed electronic state in the p-orbital basis:

$$\psi(\theta, \phi, t) = \sum_{i=1}^{3} a_i(t) p_i . \qquad (7)$$

Applying the time-dependent Schrödinger equation to the evolution of this wavefunction we obtain

$$i\hbar \dot{a}_l(t) = \sum_{m=1}^{3} a_m(t) U_{lm}(t) , \qquad (8)$$

for $l = 1, 2, 3$. U_{lm} is the matrix element of $U(t; \theta, \phi)$ in (6) between the orbitals p_l and p_m. Suppose that the integration has begun at $t = t_0$, with the initial conditions $a_k(t_0) = 1, a_{l\neq k}(t_0) = 0$. Initially, and before the system reaches regimes of strong coupling between different electronic states, $a_{l\neq k}(t)$ is bound to be very small, compatible with the fact that the atoms are propagated on $V_{kk}(\boldsymbol{r})$. At each time point, a random number ξ, $0 \leqslant \xi \leqslant 1$ is generated, and compared against $|a_{l\neq k}(t)|^2$. If

$$|a_{l\neq k}(t)|^2 > \xi , \qquad (9)$$

a transition to the electronic state l is taken to occur. The transition is modelled as an abrupt surface hopping,

and the potential surface that governs nuclear motions is changed to $V_{ll}(\boldsymbol{r}_1, \cdots, \boldsymbol{r}_N)$. At the transition, the atoms are assumed to retain their positions. All the (heavy) Kr atoms retain their momenta upon transition, as expected in the spirit of the classical limit for such a transition. The momentum of the F atom is scaled so as to yield energy conservation for the transition. The scaling is due to the momentum component in the direction for which the coupling $U_{kl}(\boldsymbol{r})$ is maximal. Upon the transition, we reset the values of the wavefunction coefficients: $a_l(t_1) = 1, a_{m\neq l}(t_1) = 0$. We propagate the atoms on the potential surface $V_{ll}(\boldsymbol{r})$, use the trajectory from this surface to obtain the time-dependent interaction (6) between the electronic states, and solve Eq. (8) in time with the above mentioned initial conditions. We will discuss elsewhere the different possible variants of the above method, e.g. the use of crude diabatic or of adiabatic states [20], the possible choices of other conditions for the electronic transition, the initialization of the trajectory after a jump, etc. We also leave for another framework the discussion of the (relatively small) differences with Tully's [23] approach and the comparison of the two algorithms. The indications are, however, that the method used here is at least semi-quantitatively reliable for this system. The results for observables will not change much if we use, e.g. the adiabatic representation. We used the method here primarily to assess the validity of the adiabatic approximation.

4. Results and discussion: F in solid Kr at thermal conditions

The results presented in this Section are for an initial state in which the F atom is at an interstitial site of the fcc Kr lattice, and the system was equilibrated at a given temperature. The dynamics was studied at three temperatures: T = 12, 25 and 75 K. The main results are as follows:

(a) *Spectroscopy.* Energy spectra for the transitions between the different electronic states of the F atom in the matrix were calculated both in the adiabatic and in the non-adiabatic scheme. It should be emphasized that the spectrum discussed here is essentially an energy spacing distribution between the two electronic states involved. It does not correspond directly to an experimentally observed spectrum. Indeed the IR transitions

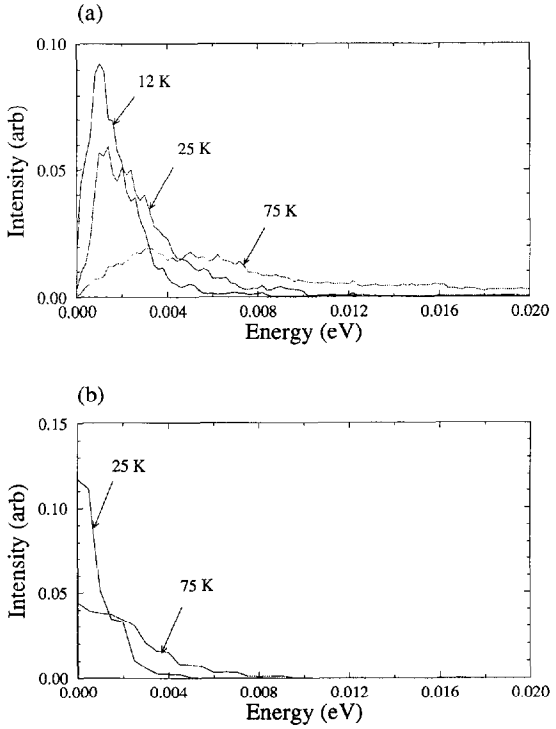

Fig. 3. (a) Electron energy spectrum for the $0 \rightarrow 1$ band of F in Kr from adiabatic simulation. (b) Electronic absorption spectrum from non-adiabatic simulation.

between the levels involved are symmetry forbidden. The transitions may be activated in the real system by mixing with excited charge-transfer electronic states, i.e. by induced dipoles or quadrupoles, depending on the local symmetry. These mechanisms will, however, affect the intensities, and no attempt was made here to model this. The calculations were carried out as for direct absorption or emission. The frequencies are, however, relevant also for the Raman case. In the adiabatic approach, the system is propagated on the lowest adiabatic potential surface, and at random time points after equilibration the vertical difference between the ground and the excited potentials is calculated at the corresponding configuration of the system. This gives the frequency of the transition. The intensity is proportional to the total time the system has spent at that configuration. The results for the $0 \rightarrow 1$ electronic absorption band is shown in Fig. 3a. The main point is that although the adiabatic potentials are degenerate for the perfect lattice configuration, *there is a dynamical*

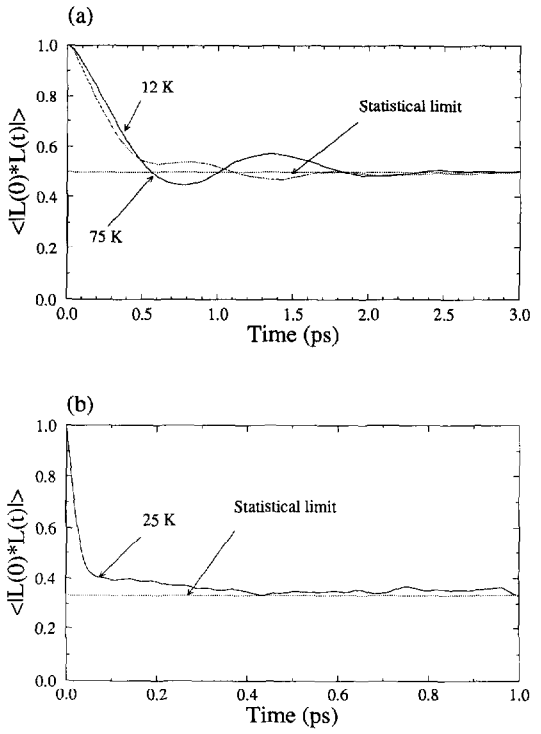

Fig. 4. (a) Correlation function for orbital orientation versus time. Adiabatic calculation. (b) Correlation function for orbital orientation versus time. Non-adiabatic calculation.

level splitting due to the excursions of the atoms away from the exact symmetry configuration. As expected, the spectrum is broader at higher T, because the excursions are of higher amplitude. The results for the $0 \rightarrow 2$ band are qualitatively very similar. Fig. 3b shows the absorption intensities from the non-adiabatic simulation. In this case, even if we select the initial electronic state, say at the ground state, the system will populate all the electronic surfaces, due to the electronic transition. Comparison of Figs. 3a and 3b suggests that the adiabatic spectra have some correct qualitative features, such as the peak position (very roughly) and the temperature effect, but are wrong on important details because the effects of hopping between surfaces can play a major role in this system.

(b) *Orbital reorientation dynamics.* Fig. 4a shows the autocorrelation function for the electronic orbital reorientation, computed in the adiabatic approximation. The correlation function $\langle |\boldsymbol{L}(t)\cdot\boldsymbol{L}(0)| \rangle$ is defined in terms of a unit vector $\boldsymbol{L}$, *chosen to have a direction along the axis of maximal electron density.* A fast ($t \lesssim 0.4$ ps) and a slower, oscillatory decay are seen. The decay is to a value of 0.5, found to be the *statistical* limit of the correlation function. (This limit is obtained, for the adiabatic case, by calculating the orientational average between a rotor and a given axis). The initial decay in Fig. (4a) is due to adiabatic "orbital following", which leads to reorientation as the F atom in its cage vibrations approaches different Kr atoms. The oscillations were found to be due to coupling between the electronic orbital and a particular asymmetric cage vibration, that has a distortion leading to an anisotropy that by Eq. (2) implies a strong torque for orbital reorientation. The amplitudes of the oscillations of the correlation function decrease with T, since at higher T the distortions are greater and the stronger coupling also with other types of distortion has an attenuation effect. Fig. 4b shows the decay of the same correlation function in the non-adiabatic calculation. Also in this case the limit to which the correlation function decays is the statistical limit, but the value of this limit is different from the adiabatic case, since in Fig. 4b three electronic states are involved. The behavior of the correlation function calculated non-adiabatically is very different from that seen in the adiabatic case: there is an initial, very fast decay ($t \lesssim 20$ fs), followed by a much slower decay ($t \lesssim 0.4$ ps). The oscillatory, long time regime of the adiabatic case is not found. Detailed analysis of the solutions shows that *the very short time reorientation in Fig. 4b occurs by a very different mechanism from the adiabatic case, and is governed by transitions between different electronic states.* On the other hand, the second time domain 0.02 ps $< t <$ 0.4 ps probably involves correlation function decay by a mechanism similar to the adiabatic (orbital following as the F approaches different Kr atoms). The decay in the non-adiabatic calculation is too strong for the long-time oscillations to survive. In conclusion, the *adiabatic approximation is in serious error for part of the time domain over which the orbital orientation decays, although a regime where it provides the main mechanism exists.*

(c) *Orientational distribution of the orbital in the cage.* Fig. 5 shows the orientational distribution of the p-orbital of the F atom in the matrix. While we do not show here two dimensional distributions in (θ, ϕ) on the unit sphere, inspection of the numerical data shows that the peaks do indeed correspond to the O_h symmetry

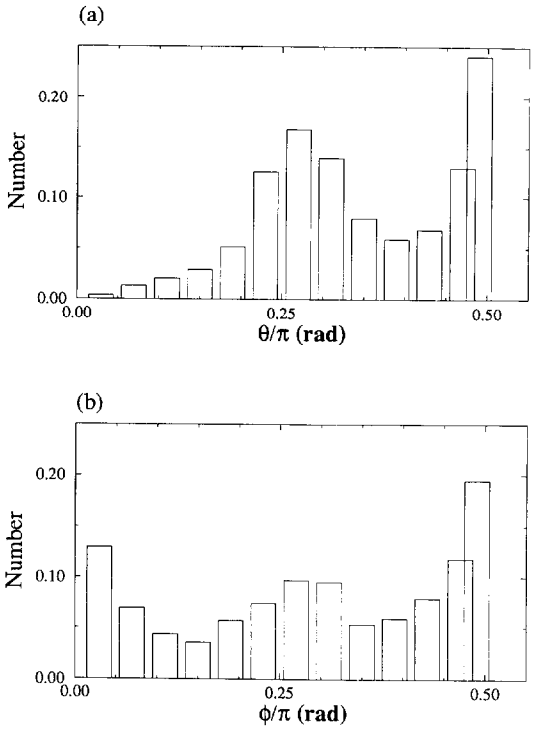

Fig. 5. (a) Orientational distribution of the F orbital in the cage: The polar angle θ dependence. (b) As in (5a), but for the azimuthal angle ϕ.

of the site. The result is for a lattice at thermal equilibrium ($T=12$ K), but with only the lowest electronic adiabatic state populated. The calculations were done in the adiabatic approximation. The distribution of the electronic orbital is clearly anisotropic. The peaks of the histograms correspond to complexes of the F(^{2}P) atom with one of the neighboring Kr atoms, in which case the p-orbital has the appropriate orientation. The result shows the strongly anisotropic nature that p-orbital states can have even when placed in a relatively isotropic cage.

(d) *Migration.* No migration of the F atom from the substitutional site was found even at 75 K over the timescale of the simulation ($t\approx 20$ ps) either in the adiabatic or in the non-adiabatic framework.

5. Results and discussion: radiative dissociation of the $Kr_2^+F^-$ exciplex in Kr

Charge-transfer absorption of F atoms in Rg solids leads to the formation of the $Rg_2^+F^-$ exciplex [27,28]. This complex relaxes by radiation, and as the Franck–Condon region corresponds to a repulsive potential region of the (ground state) Rg_2F system, the latter undergoes dissociation. We carried out simulations of the dynamics following the dissociation of Kr_2F in solid Kr. The main focus was on whether F atom migration to new sites can be induced by this dissociation. Both adiabatic and non-adiabatic calculations, as described in Section 3, were carried out. The topic is closely related to photodissociation, and subsequent atom migration, of small molecules in rare gas solids and several such processes were studied by MD simulations in recent years [29–34]. In two of these studies, the photodissociation of F_2 in Ar and in Kr was investigated, including the issue of cage exit and subsequent migration of the F atom following photolysis [32,33]. These studies were strictly in the Born–Oppenheimer framework. However, in an effort to interpret experimental data on the quantum yield for photolysis of F_2 in Kr, a heuristic model was used to represent the orientation effect of the p-orbital on the F/Kr interaction potential [33]. The improved quantitative agreement so obtained suggests that the anisotropic aspect of the interaction may play a role in the migration of F in solid Kr. One of our objectives is to explore this more rigorously, using both the adiabatic approximation and the simulations that incorporate electronic transitions. In the photolysis of F_2, the F atom produced has a large amount of kinetic energy that can overcome the barrier to cage exit and short-range migration. When Kr_2F dissociates following radiative emission of $Kr_2^+F^-$, most of the repulsive energy in the ground state of the system is along the Kr–Kr coordinate, and the kinetic energy of the F atom is only about 0.2 eV. One expects, however (and there is) a "kinetic heating" of the cage due to the released Kr–Kr repulsion energy. It is interesting to investigate whether this suffices to induce F atom migration. In simulating the initial state of the process, we used the ab initio calculations from the data of Wadt and Hay [35] for the geometry of $Kr_2^+F^-$. This exciplex was assumed to relax and equilibrate in the solid cage before undergoing radiation to the ground state of Kr_2F. Assuming a vertical transition, the initial configurations for the MD simulations were readily obtained. We proceed to discuss the results.

(a) *Photoinduced migration in the adiabatic approximation.* Fig. 6 shows the distribution of distances between the F atom position 4 ps after the Kr_2F

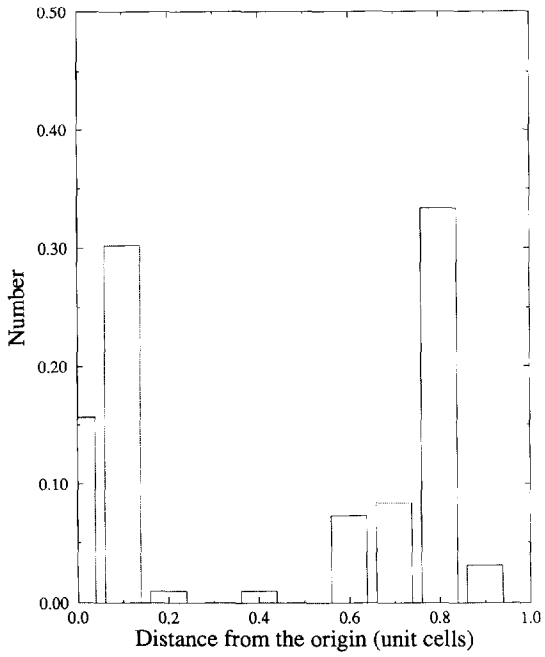

Fig. 6. Distribution of distances of F atoms from the initial position, 4 ps after the dissociation of $Kr_2^+ F^-$ in Kr.

dissociation, and the initial position of the F atom in the cage. The initial position was found to approximate, although not exactly, an interstitial O_h site. This distribution is found to be due to the fact that migration occurs to nearby sites, these being both O_h and T_d sites. The "cage heating" effect upon the dissociation of Kr_2F discussed above thus suffices to bring about migration. The total probability of migration following the dissociation in the adiabatic calculation is very high – about 50%! Typical trajectories that lead to migration and that fail to result in migration, are shown in Fig. 7. We note that the migration is relatively slow. The situation after 4 ps is essentially already stabilized.

(b) *Site-selective spectroscopy.* The difference energy distribution of F atoms in T_d and in O_h sites is shown in Fig. 8. The two spectral bands are almost non-overlapping. The important implication of this result is that *it should be possible to monitor experimentally the migration of F atoms into different sites.*

(c) *Effect of electronic transitions on F atom migration.* The results of the simulations with electronic transitions for the dissociation of Kr_2F in solid Kr are shown in Fig. 9. These results show the distribution of distances of the F atom 4 ps after dissociation from the initial position of the atom. The striking result is that *the migration probability is very small, 50 times smaller than the adiabatic one*! The reason for the difference was found to be *transfer of F atom kinetic energy into electronic excitation energy upon cage exit in the non-adiabatic simulation.* As a result the F atom is left with too little translational energy in most trajectories for surmounting the barrier for diffusion. This is reflected in Fig. 10, which shows the kinetic energy of the F atom versus time in both the adiabatic and non-adiabatic calculations. On the whole, the adiabatic approximation gives roughly the correct variation of kinetic energy with time. However, it makes an error in a particular time interval, around 0.8 ps, where translational to electronic energy transfer occurs in the non-adiabatic case, and this is exactly the "time window" critical for surmounting the barrier for migration. In conclusion, electronic transitions can have a critical effect, at least in some cases, on p-orbital atom migration, while the overall kinetic energy cooling of a hot atom is represented roughly correctly in the adiabatic framework. Finally, we note that although the non-adiabatic effects reduce greatly the occurrence of migration following photolysis, the effect still exists. Migration of F atoms induced by radiative dissociation of exciplexes has been shown in multiply doped matrices, e.g. in crystalline solid Ar doped simultaneously with F, Xe and Kr [28]. In such solids, by proper choice of excitation wavelengths, it is possible to shuttle F atoms between different scavenger centers (Xe and Kr in this case [28]). The initial kick to the F atoms in this case is due to the radiative dissociation of the diatomic Rg^+F^- via the $C \rightarrow A$ transitions. This kick, due to the repulsive RgF(A) surface, is quite different from the one simulated here. Photomobility induced by radiative dissociation of a triatomic exciplex has been most clearly demonstrated in F/Ar crystals to lead to long-range migration [28]. Indeed, the terminal Rg_2F configurations reached by radiation of Kr_2F and Ar_2F are quantitatively different. While in the first, most of the excess energy is along Kr–Kr [28], in the case of Ar_2F, based on spectral inversions, the neutral fragment is created with ~ 1 eV along Ar–Ar and ~ 0.74 eV along Ar_2–F coordinates. This excess energy should lead to significantly higher mobility of F/Ar, as verified experimentally [28].

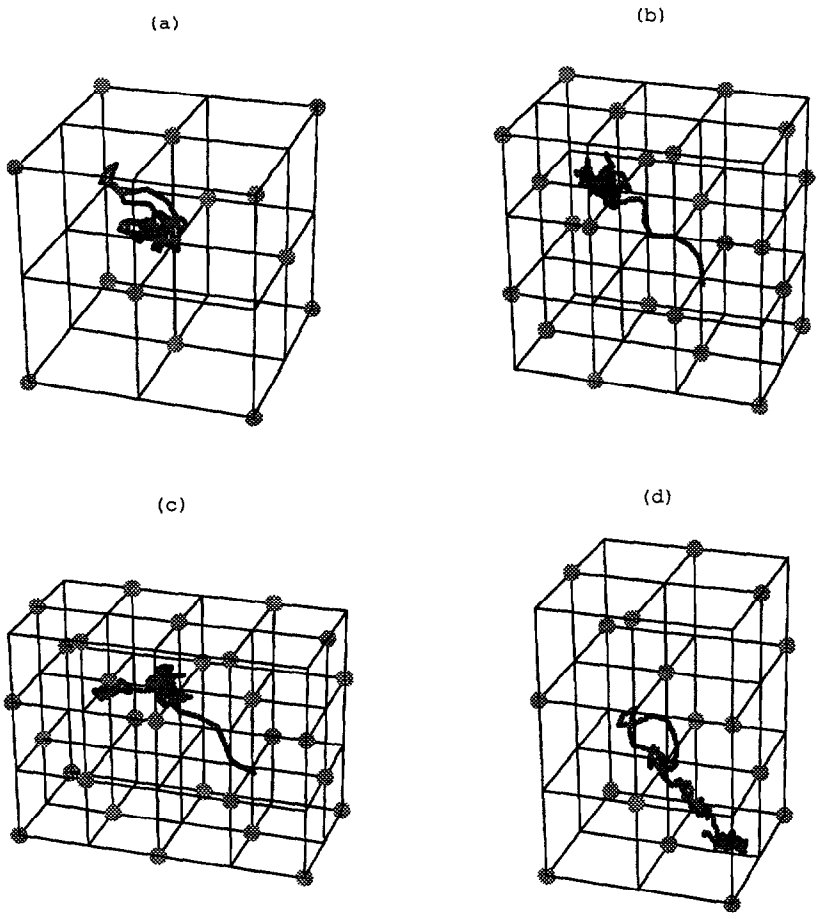

Fig. 7. Typical adiabatic trajectories for the dissociation of Kr_2F in a Kr matrix. The path of the F atom is shown. (a) No cage exit; (b) direct cage exit with stabilization in the O_h interstitial site; (c) Direct cage exit with stabilization at T_d interstitial site: (d) Indirect cage exit.

6. Concluding remarks

In this article we studied the dynamics of a p-state atom, $F(^2P)$, in a solid medium consisting of chemically inert, spherical atoms. We explored the behavior of the system at thermal conditions, and also following dissociation of an exciplex in the solid, which can provide an initial impulse for migration. It was found that the orientation, or anisotropy, of the p-orbital plays a major role in the dynamics of the system. It was shown that there are some properties that can be described by the adiabatic approximation, in which case p-orbital reorientation occurs only through "adiabatic following" of the nearby rare-gas atoms. For many properties, however, the adiabatic approximation breaks down quite severely. Thus, the adiabatic approximation describes roughly the electronic absorption frequencies and bandwidths of the open shell atom in the solid. It also describes a limited part of the orbital reorientation behavior in time, and the overall pattern of the cooling in time of a hot open-shell atom in the solid. On the other hand, the adiabatic approach is inadequate for understanding, e.g., the short-time behavior of p-orbital reorientation that in the present case is due to non-adiabatic transitions. The adiabatic approach was also found to be in dramatic error for migration of F atoms following dissociation of Kr_2F in the solid. Kinetic to electronic energy transfer was found in this case to reduce migration by a factor of 50!

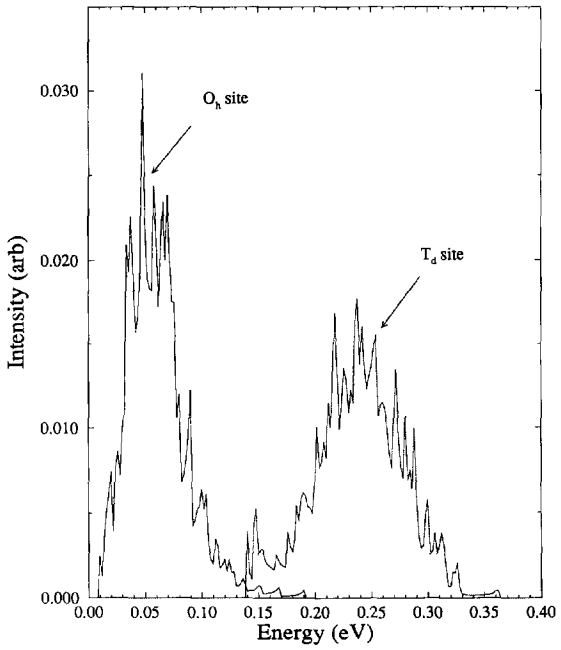

Fig. 8. Absorption lineshapes of F atoms at O_h and at T_d interstitial site in Kr.

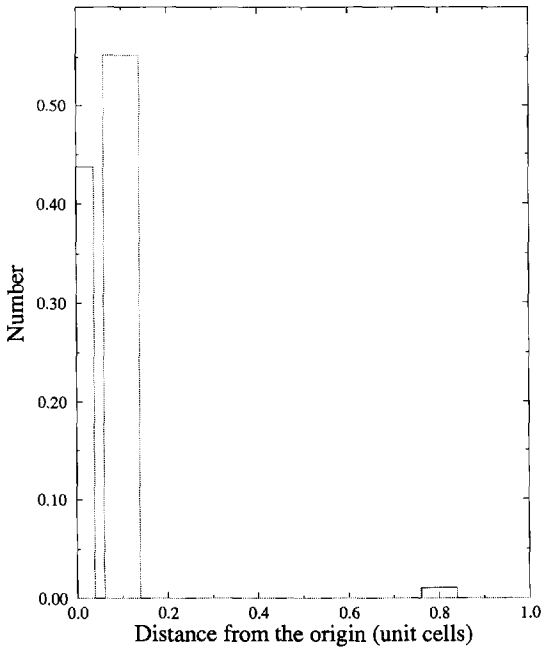

Fig. 9. Distribution of the distance of F atoms from the initial position, 4 ps after dissociation of Kr_2F. *The result is from non-adiabatic simulations*. The distances are in lattice constant units.

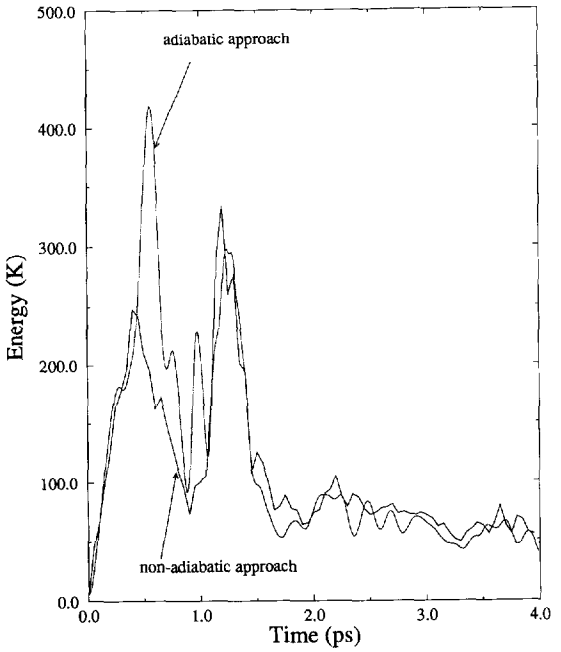

Fig. 10. Kinetic energy versus time of F atom following dissociation of Kr_2F in Kr. Results of the adiabatic and non-adiabatic calculations are shown.

The physical insights gained, and the methods employed, should be very useful for future studies of the combined dynamics of electronic and nuclear degrees of freedom in dense media.

Acknowledgement

A.I.K. and R.B.G. thank Professor R.D. Coalson for helpful discussions. The Fritz Haber Research Center at the Hebrew University is supported by the Minerva Gesellschaft für die Forschung, mbH, Munich. A.I.K. gratefully acknowledges a Graduate Fellowship from the Hebrew University. This research was supported in part by the AFOSR, under a University Research Initiative at U.C., Irvine, and by the US Air Force Phillips Laboratory under contract F29601-92K-0016.

References

[1] F. Forstmann, D.M. Kolb, D. Leutloff and W. Schulze, J. Chem. Phys. 66 (1977) 2806.

[2] H. Wiggenhauser, W. Schroeder and D.M. Kolb, J. Chem. Phys. 88 (1988) 3434.
[3] T. Hebert, H. Wiggenhauser, U. Schriever and D.M. Kolb, J. Chem. Phys. 92 (1990) 1575.
[4] A. Stangassinger, J. Sheuchenflug, T. Priz and V.E. Bondybey, Chem. Phys. 178 (1993) 204.
[5] M.E. Fajardo and P.G. Carrick, J. Chem. Phys. 94 (1991) 5812.
[6] M.E. Fajardo, J. Chem. Phys. 98 (1993) 110.
[7] H. Kunttu, E. Sekreta and V.A. Apkarian, J. Chem. Phys. 94 (1991) 7819.
[8] (a) A. Danilychev, R. Zadoyan, W.G. Lawrence, in: Proceedings of the High Energy Density Matter Conference (Woods Hole, MA, 1993); US Air Force Material Command (1993) p. 54;
(b) A.V. Danylichev and V.A. Apkarian, J. Chem. Phys. 100 (1994) 5556;
(c) W.G. Lawrence and V.A. Apkarian, J. Chem. Phys. 101 (1994) 1.
[9] L.C. Balling and J.J. Wright, J. Chem. Phys. 79 (1983) 2941.
[10] M.E. Fajardo, J. Chem. Phys. 98 (1993) 119.
[11] J.A. Boatz and M.E. Fajardo, Proceedings of the High Energy Density Matter Contractors Conference (Lancaster, CA, 1992). US Air Force Office of Scientific Research (1992) p. 230.
[12] J.P. Visticot, P. de Pujo, J.M. Mestdagh, A. Lallement, J. Berlande, O. Sublemontier, P. Meynadier and J. Cuvellier, J. Chem. Phys., in press.
[13] I. Benjamin and K.R. Wilson, J. Chem. Phys. 90 (1989) 4176.
[14] I.M. Gersonde and H. Gabriel, J. Chem. Phys. 98 (1992) 2094.
[15] R.H. Aziz and M.J. Slaman, Mol. Phys. 58 (1986) 679.
[16] C.H. Becker, P. Casavecchia and Y.T. Lee, J. Chem. Phys. 70 (1979) 2986.
[17] P. Casavecchia, in: Dynamics of polyatomic van der Waals complexes, eds. N. Halberstadt and K.C. Janda (Plenum Press, New York, 1990) p. 123.
[18] V. Aquilanti and G. Grossi, J. Chem. Phys. 73 (1980) 1165.
[19] V. Aquilanti, P. Casavecchia, G. Grossi and A. Lagana, J. Chem. Phys. 73 (1980) 1173.
[20] A.I. Krylov, R.B. Gerber and R.D. Coalson, to be published.
[21] H.D. Meyer and W.H. Miller, J. Chem. Phys. 70 (1979) 3214.
[22] L.J. Dunne, J.N. Murrell and J.G. Stamper, Chem. Phys. Letters 112 (1984) 497.
[23] J.C. Tully, J. Chem. Phys. 93 (1990) 1061.
[24] P.J. Kuntz, J. Chem. Phys. 95 (1991) 141.
[25] F. Webster, P.J. Rossky and R.A. Freisener, Computer Phys. Commun. 63 (1991) 494.
[26] E. Neria, A. Nitzan, R.N. Barnet and U. Landman, Phys. Rev. Letters 67 (1991) 1011.
[27] H. Kunttu, J. Feld, R. Alimi, A. Becker and V.A. Apkarian, J. Chem. Phys. 92 (1990) 4856.
[28] J. Feld, H. Kunttu and V.A. Apkarian, J. Chem. Phys. 93 (1990) 1009.
[29] R. Alimi, R.B. Gerber and V.A. Apkarian, J. Chem. Phys. 89 (1988) 174.
[30] R.B. Gerber, R. Alimi and V.A. Apkarian, Chem. Phys. Letters 158 (1989) 257.
[31] R. Alimi, A. Brokman and R.B. Gerber, J. Chem. Phys. 91 (1989) 1611.
[32] R. Alimi, R.B. Gerber and V.A. Apkarian, J. Chem. Phys. 92 (1990) 3551.
[33] R. Alimi, R.B. Gerber and V.A. Apkarian, Phys. Rev. Letters 66 (1991) 1295.
[34] R. Alimi, R.B. Gerber, J.G. McCaffrey, H. Kunz and N. Schwentner, Phys. Rev. Letters 69 (1992) 856.
[35] W.R. Wadt and P.J. Hay, J. Chem. Phys. 68 (1978) 3850.